arXiv:0901.2477v2 [hep-ph] 26 Aug 2009

Pion condensation in a dense neutrino gas

Hiroaki Abuki,[*] Tomáš Brauner,[†] and Harmen J. Warringa[‡]
Institut für Theoretische Physik, Goethe-Universität Frankfurt,
Max-von-Laue-Straße 1, 60438 Frankfurt am Main, Germany

(Dated: August 26, 2009)

We argue that using an equilibrated gas of neutrinos it is possible to probe the phase diagram of QCD for finite isospin and small baryon chemical potentials. We discuss this region of the phase diagram in detail and demonstrate that for large enough neutrino densities a Bose-Einstein condensate of positively charged pions arises. Moreover, we show that for nonzero neutrino density the degeneracy in the lifetimes and masses of the charged pions is lifted.

I. INTRODUCTION

Quantum chromodynamics (QCD) predicts that the properties of hadronic matter hugely depend on the baryon and isospin density. For example, it is found that for small baryon chemical potential such that there are no baryons around a Bose-Einstein condensate of charged pions should arise if the absolute value of the isospin chemical potential (μ_I) becomes larger than the vacuum pion mass (m_π) [1]. This has been shown using the chiral effective Lagrangian [1, 2, 3]. Furthermore the existence of a pion condensate was also demonstrated in lattice QCD [4, 5, 6, 7, 8], with random matrix theory [9], using the Nambu–Jona-Lasinio (NJL) model [10, 11, 12, 13, 14], with the $O(4)$ linear sigma model [15, 16] and with string theory inspired holographic models of QCD [17, 18, 19].

The question we would like to address in this article is under which conditions a pion condensate can be realized in a macroscopic system of particles. In order for a macroscopic system to be stable, it should be electrically neutral. Since the isospin chemical potential is equal to the charge chemical potential ($\mu_I = \mu_Q$), requiring neutrality puts restrictions to the value of the isospin chemical potential.

At low baryon chemical potential ($\mu_B \lesssim m_p$, here m_p denotes the mass of the proton), the electric neutrality constraint forces $\mu_Q \approx 0$ so that pion condensation becomes impossible [20] (see also Refs. [21, 22]). If however a finite density of neutrinos which is in equilibrium with hadronic matter is present, these considerations will be modified. As we will discuss in Sec. II a nonzero density of neutrinos always increases μ_Q. If the baryon chemical potential is small and the chemical potential of the neutrinos becomes large enough, it will be energetically favored to convert some of the neutrinos into pions and electrons. In this way as we will show in Sec. II a pion condensate is formed in a dense neutrino gas for low baryon chemical potential. This has interesting consequences for the phase diagram of QCD at finite electron and/or muon lepton number chemical potential. In Sec. II and Sec. III we will show that pion condensation takes place in a large part of the phase diagram of QCD for $|\mu_B| \lesssim m_p - m_\pi$. Even before the onset of pion condensation, the neutrino gas has interesting implications on the behavior of the pions. Because of the nonzero isospin chemical potential, the degeneracy in the masses of the charged pions will be lifted. Moreover, the lifetime of the pions will change as we will see in Sec. IV.

Let us point out that similar condensation phenomena can also arise at larger baryon chemical potential ($\mu_B \gtrsim m_p$). In dense electrically neutral nuclear matter, $-\mu_Q$ can become of the order of the vacuum pion mass. Hence condensation of negatively charged pions in dense nuclear matter seemed a realistic possibility [23, 24, 25]. However, due to interactions the in-medium pion mass in nuclear matter is increased such that pion condensation becomes improbable. On the other hand, the mass of the negatively charged kaon is decreased due to an attractive interaction. A negatively charged kaon condensate turns out to be a more likely possibility in dense neutral nuclear matter [26] even at high neutrino densities [27]. In color superconducting matter which is formed at even higher baryon densities, the masses of the kaonic excitations are smaller than those of the pionic excitations [28]. It turns out that in electrically neutral color superconducting matter a neutral kaon condensate can be formed, creating the so-called CFL-K^0 phase [29, 30, 31, 32, 33, 34, 35].

In nature a dense neutrino gas is created during a supernova explosion. Part of the neutrinos produced in this explosion will be trapped in the precursor of a neutron star, the so-called proto-neutron star [36]. Inside a proto-neutron star the baryon density is very large, which as we stated above makes pion condensation unlikely. However, one could speculate that in the crust or in the atmosphere the neutrino density might be large and baryon density small enough for pion condensation to occur. To fully settle this issue one should also show that chemical and thermal equilibrium can be reached. In this paper, we will not give a definite answer to the question whether or not a pion condensate is realized somewhere in our universe. We will only unambiguously show that a pion condensate is formed if the conditions are right, that is in a dense neutrino gas at low baryon densities.

---

[*] Electronic address: abuki@th.physik.uni-frankfurt.de
[†] Electronic address: brauner@th.physik.uni-frankfurt.de; On leave from Department of Theoretical Physics, Nuclear Physics Institute ASCR, 25068 Řež, Czech Republic.
[‡] Electronic address: warringa@th.physik.uni-frankfurt.de

II. PION CONDENSATION

At very large neutrino density and small baryon chemical potential it is energetically favored to convert some of the neutrinos into pions and leptons. In this section we will show that in such a case a pion condensate will be formed. We will compute at which neutrino density this will happen and discuss the phase diagram as a function of electron and muon lepton number chemical potential.

In order to describe matter at finite density we express the chemical potentials of the up quark (u), down quark (d), electron (e), electron neutrino (ν_e), muon (μ) and muon neutrino (ν_μ) in terms of the chemical potentials of conserved quantities. We will assume that chemical equilibrium is reached, hence

$$\begin{aligned}
\mu_u &= \tfrac{1}{3}\mu_B + \tfrac{2}{3}\mu_Q, \\
\mu_d &= \tfrac{1}{3}\mu_B - \tfrac{1}{3}\mu_Q, \\
\mu_e &= -\mu_Q + \mu_{L_e}, \\
\mu_{\nu_e} &= \mu_{L_e}, \\
\mu_\mu &= -\mu_Q + \mu_{L_\mu}, \\
\mu_{\nu_\mu} &= \mu_{L_\mu}.
\end{aligned} \tag{1}$$

Here μ_B, μ_Q, μ_{L_e} and μ_{L_μ} denote respectively the chemical potentials for baryon number, electric charge, electron lepton number and muon lepton number. Strictly speaking, the muon and electron lepton numbers are not separately conserved due to neutrino oscillations. We will assume that the size of our system is much smaller than the neutrino oscillation length. Furthermore, we will assume that the time it takes to bring the system in chemical equilibrium is much shorter than the typical neutrino oscillation time. In this situation it is to first approximation correct to introduce separate chemical potentials for electron and muon lepton numbers. On long time scales only total lepton number is conserved and one can no longer talk about separate lepton number chemical potentials. This situation is a special case of our results in which $\mu_{L_e} = \mu_{L_\mu}$.

To make the system of particles electrically neutral, the charge chemical potential has to be chosen in such a way that the charge density n_Q vanishes. This can be achieved by solving the following equation

$$n_Q = -\frac{\partial\Omega}{\partial\mu_Q} = 0, \tag{2}$$

where Ω denotes the thermodynamic potential. It has a hadronic and leptonic component. We will write

$$\Omega = \sum_{i=e,\mu} (\Omega_i + \Omega_{\nu_i}) + \Omega_h, \tag{3}$$

where Ω_h is the contribution of the hadrons, Ω_i that of charged leptons and Ω_{ν_i} that of the neutrinos. To a good approximation the leptons can be described by a free non-interacting gas of fermions. Hence the thermodynamic potential of the charged leptons is given by

$$\Omega_i = -\frac{T}{\pi^2}\sum_{\pm}\int_0^\infty \mathrm{d}p\, p^2 \log\left[1 + e^{-\beta(\omega_p \pm \mu_i)}\right], \tag{4}$$

where $\omega_p = (p^2 + m_i^2)^{1/2}$ and $\beta = 1/T$ denotes the inverse temperature. For the neutrinos (which only have left-handed chirality) one has

$$\Omega_{\nu_i} = -\frac{T}{2\pi^2}\sum_{\pm}\int_0^\infty \mathrm{d}p\, p^2 \log\left[1 + e^{-\beta(p \pm \mu_{\nu_i})}\right]. \tag{5}$$

The densities of the leptons can be found by taking the derivative of the thermodynamical potential with respect to the chemical potential. In this way for zero temperature one finds that the density of the charged leptons equals

$$n_i = \frac{1}{3\pi^2}\mathrm{sgn}(\mu_{L_i} - \mu_Q)\left[(\mu_{L_i} - \mu_Q)^2 - m_i^2\right]^{3/2}, \tag{6}$$

for $|\mu_{L_i} - \mu_Q| \geq m_i$ and $n_i = 0$ otherwise. The density of the neutrinos is equal to

$$n_{\nu_i} = \frac{1}{6\pi^2}\mu_{L_i}^3 + \frac{1}{6}\mu_{L_i}T^2. \tag{7}$$

Now let us set the temperature to zero and take μ_B small so that there are no baryons in the system. This means that the chemical potential of the proton ($\mu_p = \mu_B + \mu_Q$) should be smaller than the proton mass m_p. Since μ_Q can become m_π, this translates into the requirement that $|\mu_B| \lesssim m_p - m_\pi$. In that case it is well known from the analysis using the chiral effective Lagrangian that a π^+ condensate will form via a second-order transition if $\mu_Q > m_\pi$ [1, 2]. This is confirmed by lattice QCD simulations [4].

If in this particular situation $|\mu_Q|$ is smaller than m_π, there are no hadronic states around. Hence the hadronic sector is automatically electrically neutral. The question then is, can we neutralize the leptonic sector such that $\mu_Q = m_\pi$? If so, we have found the onset of pion condensation in electrically neutral matter. Answering this question amounts to solving the following equation

$$\sum_i n_i(\mu_Q = m_\pi) = 0. \tag{8}$$

If there are no neutrinos around this equation has no solution since $\mu_Q = m_\pi$ automatically introduces a nonzero density of electrons and muons. However, if we for example take $\mu_{L_e} = \mu_{L_\mu} \equiv \mu_L$ we find that $\mu_Q = \mu_L$ guarantees electric neutrality. Pion condensation then sets in at $\mu_L = m_\pi$. This corresponds to a electron and muon neutrino number density of $m_\pi^3/(6\pi^2) \approx 5.9 \times 10^{-3}$ fm^{-3}.

A. Phase diagram μ_{L_e} vs. μ_{L_μ} at $T = 0$

Now that we found the onset of pion condensation in electrically neutral matter for equal electron and muon

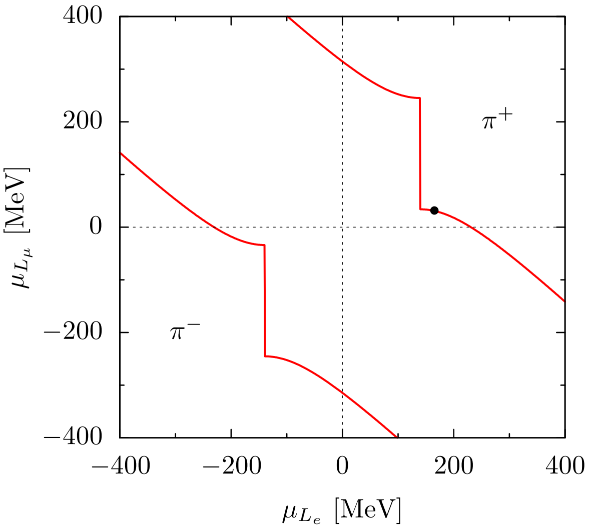

FIG. 1: Phase diagram of electrically neutral QCD at $T = 0$, valid for $|\mu_B| \lesssim m_p - m_\pi$, as a function of the electron and muon lepton number chemical potential. The phase boundary denotes a second-order transition. The black dot denotes the point where $n_{L_\mu} = 0$.

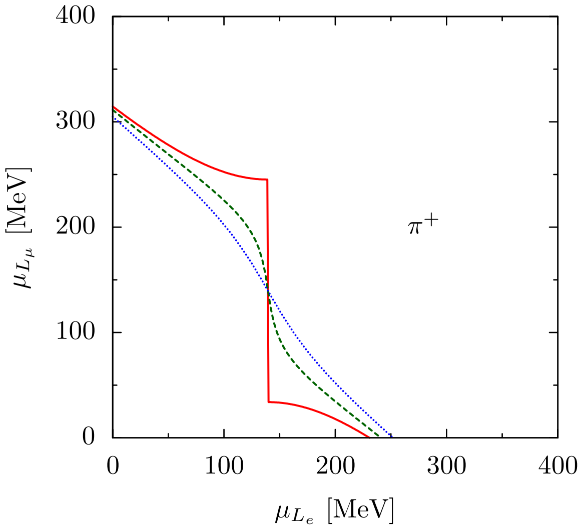

FIG. 2: Phase diagram of electrically neutral QCD, valid for $|\mu_B| \lesssim m_p - m_\pi$, for $T = 0$ (solid, red), 25 (dashed, green), and 50 MeV (dotted, blue), as a function of the electron and muon lepton number chemical potential. The $T = 25$ and 50 MeV results are estimates.

lepton number chemical potential, let us see what happens in the more general case in which they are different. By solving Eq. (8) for $\mu_Q = m_\pi$ we obtain the phase diagram of QCD as a function of μ_{L_e} and μ_{L_μ} for $T = 0$ and small baryon chemical potential. We display the result in Fig. 1.

Let us discuss the transition line to the π^+-condensed phase in somewhat more detail. If $m_\pi - m_\mu < \mu_{L_\mu} < m_\pi + m_\mu$ there are no muons in the system so it should be neutralized solely by the electrons. This then gives $m_\pi - m_e < \mu_{L_e} < m_\pi + m_e$ which corresponds to the vertical lines in the phase diagram of Fig. 1. Hence the length of the vertical line is equal to twice the muon mass. For $\mu_{L_e} < m_\pi - m_e$ the exact solution to the neutrality constraint gives the following phase boundary

$$\mu_{L_\mu} = m_\pi + \sqrt{(\mu_{L_e} - m_\pi)^2 - m_e^2 + m_\mu^2}. \qquad (9)$$

while for $\mu_{L_e} > m_\pi + m_e$ we find

$$\mu_{L_\mu} = m_\pi - \sqrt{(\mu_{L_e} - m_\pi)^2 - m_e^2 + m_\mu^2}. \qquad (10)$$

If the muon lepton number chemical potential vanishes, a π^+ condensate will form if

$$\mu_{L_e} > m_\pi + \sqrt{m_\pi^2 + m_e^2 - m_\mu^2} = 231 \text{ MeV}. \qquad (11)$$

This corresponds to an electron neutrino density of $\mu_{L_e}^3/(6\pi^2) = 2.7 \times 10^{-2}$ fm^{-3}.

In some situations like the proto-neutron star it is natural to require zero muon lepton number density ($n_{L_\mu} = n_\mu + n_{\nu_\mu} = 0$). In such a case we find that the transition to the pion condensed phase occurs at

$$\mu_{L_\mu} = \xi m_\pi - \xi\sqrt{m_\pi^2 + (m_\mu^2 - m_\pi^2)/\xi} = 31 \text{ MeV}, \qquad (12)$$

here $\xi = 1/[1-(1/2)^{2/3}]$. The electron chemical potential is then equal to

$$\mu_{L_e} = m_\pi + \sqrt{(\tfrac{1}{2})^{2/3}\mu_{L_\mu}^2 + m_e^2}. \qquad (13)$$

To a good approximation we can neglect the electron mass in the last equation. Then by expanding Eq. (12) in powers of $(m_\pi^2 - m_\mu^2)/m_\pi^2$ we obtain

$$\mu_{L_e} \approx m_\pi \left(1 + \frac{1}{2^{4/3}} \frac{m_\pi^2 - m_\mu^2}{m_\pi^2}\right) = 164 \text{ MeV}. \qquad (14)$$

The solution using the exact expression gives $\mu_{L_e} = 163$ MeV. Hence if the muon lepton number density vanishes pion condensation will occur if the electron neutrino density is larger than $\mu_{L_e}^3/(6\pi^2) = 9.6 \times 10^{-3}$ fm^{-3}.

B. Phase diagram μ_{L_e} vs. μ_{L_μ} for $T \ll m_\pi$

Let us now discuss how the μ_{L_e} vs. μ_{L_μ} phase diagram of electrically neutral QCD looks like at finite temperature. As long as the temperature is much smaller than the chiral phase transition temperature T_c, the mass of the pion is not much different from the vacuum pion mass m_π. Hence for $T \ll T_c$ the onset of pion condensation still occurs to a good approximation at $\mu_Q = m_\pi$.

If the temperature is also much smaller than m_π, there are to a good approximation no hadronic states in the system as long as $\mu_Q < m_\pi$. Hence we can like in the previous subsection find the onset of pion condensation by solving Eq. (8), but now at finite temperature. We display the results in Fig. 2.

To understand Fig. 2 better, let us see what happens if the temperature is increased. In that case the muon mass, which is equal to half of the length of the vertical line in the phase diagram, becomes less important. Let us for a moment neglect the muon mass completely. Then the solution of Eq. (8) is a straight line from $(\mu_{L_e}, \mu_{L_\mu}) = (2m_\pi, 0)$ to $(0, 2m_\pi)$. At these high temperatures where the muon mass can be neglected, the approximation of ignoring the hadrons is wrong, so that the straight line will never be the real phase boundary. Nevertheless, this argument shows that by raising the temperature the tendency of the phase boundary is to approach the straight line as long as $T \ll m_\pi$ in agreement with the results displayed in Fig. 2. As a result of this straightening tendency there are points in the phase diagram ($\mu_{L_e} < m_\pi$, $\mu_{L_\mu} > m_\pi$) where the pion condensate does not appear at $T = 0$ but arises if the temperature is increased.

III. NJL MODEL CALCULATION

As was shown in the previous section, pion condensation arises in electrically neutral hadronic matter for large neutrino densities. We have obtained the phase diagram of QCD for low temperatures and small baryon chemical potential. It is of interest to see what happens to the phase diagram at larger baryon chemical potential and higher temperatures.

To investigate the phase diagram at finite T and μ_B we need to know the hadronic component of the thermodynamic potential, Ω_h. Unfortunately we can not compute Ω_h in QCD from first principles. We will resort to an effective model of QCD, the Nambu–Jona-Lasinio (NJL) model (see e.g. Ref. [37] for an extensive review). The NJL model qualitatively describes QCD. It for example captures the chiral phase transition and can be used to study mesons and pion condensation. However, it is important to realize that nuclear matter is not described at all with this model. The phase diagrams obtained with the NJL model will therefore only describe the qualitative features of the QCD phase diagram. Nevertheless, as we argued in the previous section, our conclusion that a large part of the phase diagram contains the pion condensate is certainly also correct for QCD.

The 2-flavor NJL model we will use in this article is given by the following Lagrangian density

$$\begin{aligned}
\mathcal{L} &= \bar{\psi}\left(i\gamma^\mu\partial_\mu - m + \mu\gamma_0\right)\psi + (1-\alpha)\mathcal{L}_1 + \alpha\mathcal{L}_2, \\
\mathcal{L}_1 &= G[(\bar{\psi}\psi)^2 + (\bar{\psi}\vec{\tau}\psi)^2 + (\bar{\psi}i\gamma_5\psi)^2 + (\bar{\psi}i\gamma_5\vec{\tau}\psi)^2], \\
\mathcal{L}_2 &= G[(\bar{\psi}\psi)^2 - (\bar{\psi}\vec{\tau}\psi)^2 - (\bar{\psi}i\gamma_5\psi)^2 + (\bar{\psi}i\gamma_5\vec{\tau}\psi)^2].
\end{aligned} \tag{15}$$

Here G is the coupling constant and $\vec{\tau}$ denotes the Pauli matrices. The mass matrix m is diagonal and contains the bare quark masses m_u and m_d. The matrix μ is also diagonal and contains the quark chemical potentials μ_u and μ_d, which are given in Eq. (1). The interaction terms $\mathcal{L}_1$ and $\mathcal{L}_2$ are invariant under $\mathrm{SU(2)_L} \times \mathrm{SU(2)_R}$ transformations, as is QCD. The interaction $\mathcal{L}_1$ preserves the axial $\mathrm{U(1)_A}$ symmetry, while $\mathcal{L}_2$ (the two-flavor 't Hooft term) breaks it. In QCD the $\mathrm{U(1)_A}$ symmetry is broken, so α should be nonzero.

Since the NJL model is an effective model which is only valid for low momenta, one has to specify an ultraviolet regularization. In this paper we will employ a three-dimensional sharp momentum cutoff Λ.

We will take the following parameter set which is also used in other papers (see e.g. Refs. [38, 39]): $G = 5.04\ \mathrm{GeV}^{-2}$, $\Lambda = 651$ MeV and $m \equiv m_u = m_d = 5.5$ MeV. We will treat α as a free parameter. At zero temperature and baryon chemical potential, its most likely value lies somewhere between 0.1 and 0.2 [37, 40]. With this parameter set one can reproduce the vacuum properties of the mesons, $m_{\pi^\pm} \approx 140$ MeV, $f_\pi \approx 92$ MeV.

In order to compute the thermodynamic potential, we will resort to the mean-field approximation. We will introduce the following mean fields

$$\begin{aligned}
\sigma_u &= -4G\langle\bar{u}u\rangle, \\
\sigma_d &= -4G\langle\bar{d}d\rangle, \\
\rho &= -2G\langle\bar{\psi}\tau_2 i\gamma_5\psi\rangle,
\end{aligned} \tag{16}$$

here σ_u and σ_d are proportional to the chiral condensates, while the pion condensate is described by ρ.

The hadronic part of the thermodynamic potential can now be found by expanding the Lagrangian density around the mean fields and integrating out the fermions. In that way one obtains

$$\begin{aligned}
\Omega_h &= \frac{\frac{1}{2}(1-\alpha)(\sigma_u^2 + \sigma_d^2) + \alpha\sigma_u\sigma_d + \rho^2}{4G} \\
&- \frac{N_c}{2\pi^2}\sum_{i=1}^{4}\int_0^\Lambda \mathrm{d}p\, p^2\left[|\lambda_i| + 2T\log\left(1 + e^{-\beta|\lambda_i|}\right)\right].
\end{aligned} \tag{17}$$

Here $N_c = 3$ denotes the number of colors and λ_i are the four independent eigenvalues of the mean-field Hamiltonian $\mathcal{H}$ which is given by

$$\mathcal{H} = \begin{pmatrix} \gamma^0\vec{\gamma}\cdot\vec{p} + M_u\gamma_0 - \mu_u & \gamma^0\gamma_5\rho \\ -\gamma^0\gamma_5\rho & \gamma^0\vec{\gamma}\cdot\vec{p} + M_d\gamma_0 - \mu_d \end{pmatrix}, \tag{18}$$

where the constituent quark masses are equal to

$$\begin{aligned}
M_u &= m_u + (1-\alpha)\sigma_u + \alpha\sigma_d, \\
M_d &= m_d + (1-\alpha)\sigma_d + \alpha\sigma_u.
\end{aligned} \tag{19}$$

If $M_u = M_d \equiv M$ the four eigenvalues can be obtained analytically and read

$$\lambda_i = \sqrt{(\omega_p \pm \mu_Q/2)^2 + \rho^2} \pm \bar{\mu} \tag{20}$$

where $\bar{\mu} = \mu_B/3 + \mu_Q/6$ and $\omega_p = \sqrt{p^2 + M^2}$. The values of the mean fields follow by minimizing the thermodynamic potential with respect to these mean fields,

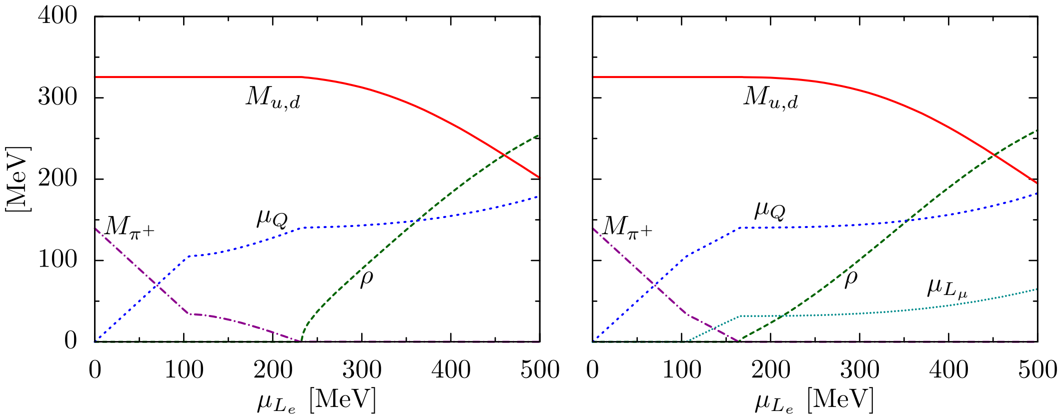

FIG. 3: Evolution of the condensates and chemical potentials along the $\mu_B = 0$ axis at zero temperature. Left panel: The $\mu_{L_\mu} = 0$ case. Right panel: The $n_{L_\mu} = 0$ case. Displayed are: constituent quark mass (red, solid), pion condensate (green, long-dashed), electric charge chemical potential (blue, short-dashed), in-medium π^+ mass (magenta, dash-dotted), and muon lepton number chemical potential (cyan, dotted). The in-medium pion mass is discussed in Sec. IV A.

which amounts to solving the following equations

$$\frac{\partial\Omega}{\partial\sigma_u} = \frac{\partial\Omega}{\partial\sigma_d} = \frac{\partial\Omega}{\partial\rho} = 0. \tag{21}$$

In addition one has to solve the electric neutrality constraint, Eq. (2), and in the case where we require zero muon lepton number density, also the constraint $n_{L_\mu} = 0$. If $\alpha = 1/2$, the effective potential is a function of $\sigma_u + \sigma_d$. Hence in that case one always finds $\sigma_u = \sigma_d$ as a solution. For other values of α, σ_u and σ_d can be different.

We have solved Eq. (21) and the neutrality constraints numerically and will discuss the results in the following subsections.

A. Condensates at $T = 0$ and $\mu_B = 0$

In Fig. 3 we show the results achieved at zero temperature and baryon chemical potential. In this limit the condensation is governed by the chiral physics and the NJL model, augmented with the gas of free leptons to account for charge neutrality, is therefore expected to be most reliable.

First of all, note that the NJL calculation naturally reproduces the previous model-independent evaluation of the onset of pion condensation. To demonstrate that even the quantitative results inside the pion-condensed phase are to a large extent model-independent, one can employ chiral perturbation theory [1, 2]. The leading-order (Euclidean) chiral Lagrangian reads

$$\mathcal{L}_{\chi\mathrm{PT}} = \frac{f_\pi^2}{4}\left[\mathrm{Tr}(D_\mu U^\dagger D_\mu U) - 2m_\pi^2 \mathrm{Re}\,\mathrm{Tr}U\right], \tag{22}$$

where U is a unitary 2×2 matrix field and the covariant derivative, $D_\mu U = \partial_\mu U - \ell_\mu U + U r_\mu$, incorporates its coupling to external left- and right-handed vector fields, ℓ_μ and r_μ. In presence of electric charge or isospin chemical potential, they are $\ell_0 = r_0 = \frac{1}{2}\tau_3\mu_Q$.

The ground-state expectation value of the order parameter can be without lack of generality cast as

$$U = \begin{pmatrix} \cos\theta & \sin\theta \\ -\sin\theta & \cos\theta \end{pmatrix}. \tag{23}$$

If $\theta = 0$ we recover the vacuum chiral condensate, while $\theta = \pi/2$ would be a purely pion condensate. In general this rotation angle is determined by minimization of the static part of the Lagrangian and for $|\mu_Q| > m_\pi$ is given by [1]

$$\cos\theta = \frac{m_\pi^2}{\mu_Q^2}. \tag{24}$$

This is analogous to the gap equation in the NJL model and provides a model-independent relation among the chiral and pion condensates and the electric charge chemical potential. The electric charge density of the pion condensate is in turn obtained as [1]

$$n_\pi = -\frac{\partial\mathcal{L}_{\chi\mathrm{PT}}}{\partial\mu_Q} = f_\pi^2\mu_Q\left(1 - \frac{m_\pi^4}{\mu_Q^4}\right). \tag{25}$$

We used these expressions supplemented with the lepton sector to check the results of Fig. 3. Since chiral perturbation theory allows a straightforward evaluation of the expectation values of fermion bilinear operators rather than the NJL order parameters $\sigma_{u,d}, \rho$, see Eq. (16), we use the vacuum NJL value of $\sigma_u = \sigma_d$ to normalize the condensates obtained with chiral perturbation theory. The results agree with NJL model up to about a 2% accuracy even at the highest values of μ_{L_e} considered. Therefore, we do not plot the corresponding lines in Fig. 3; they would hardly be distinguishable. (See [13] for a similar comparison.)

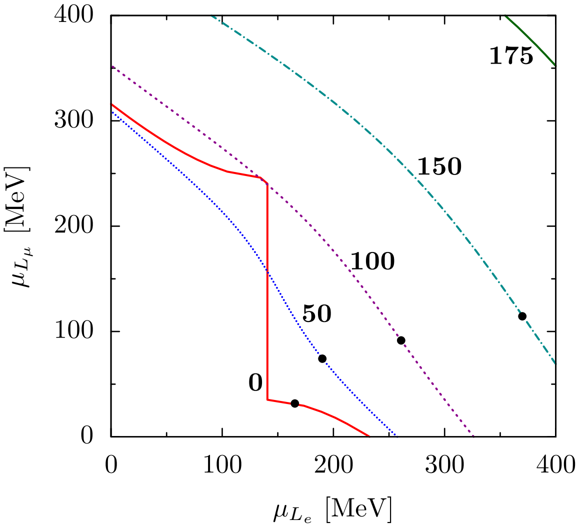

FIG. 4: Phase diagram of the electrically neutral NJL model with $\alpha = 0$ at various values of temperature (indicated by the numbers in boldface). The black dots denote the points at the different phase boundaries where the muon lepton number density (n_{L_μ}) vanishes.

B. Phase diagram μ_{L_e} vs. μ_{L_μ} at finite temperature

In Fig. 4 we display the phase diagram of the NJL model as a function of μ_{L_e} and μ_{L_μ} for different temperatures at $\mu_B = 0$ and $\alpha = 0$. We found that up to about $T = 150$ MeV this phase diagram does not change much by modifying α. Comparing this phase diagram to Fig. 2 we find very good agreement with the model-independent estimates up to $T = 50$ MeV. Hence we can say that Fig. 2 most likely represents the phase diagram of electrically neutral QCD for small baryon density as a function of lepton number chemical potentials.

For higher temperatures the NJL model calculation serves as an illustration of how the phase diagram of QCD would qualitatively look like. We find that the onset of the pion condensed phase moves to higher values of the lepton number chemical potentials. This is caused by the appearance of charged hadronic states in the system which affects the neutrality. Furthermore due to the increase of the pion mass at finite temperature, the onset of pion condensation moves to larger values of μ_Q.

C. Phase diagram μ_B vs. μ_L at zero temperature

In Ref. [41] the phase diagram of neutral matter with neutrinos present was discussed for very large baryon chemical potential where color superconducting phases arise. See also Refs. [42, 43]. Here we complement this phase diagram with the results obtained at low baryon chemical potential. We display the results in Fig. 5 for the two cases regarding the muon-lepton content discussed above, and for two different values of the α parameter.

The structure of the phase diagram is simple. The straight line, which determines the onset of pion condensation at low baryon chemical potential, is given by the model independent argument presented in Sec. II. The corner of the pion condensed phase, where this line breaks, is marked by the appearance of up quarks in the system. In the NJL model at the mean-field approximation, quarks behave as noninteracting quasiparticles with effective energy gap (mass) determined by $M_{u,\text{eff}} = M_u - \frac{1}{3}\mu_B - \frac{2}{3}\mu_Q$, $M_{d,\text{eff}} = M_d - \frac{1}{3}\mu_B + \frac{1}{3}\mu_Q$. When this drops below zero, a Fermi sea of quarks is formed. This happens along the boundary of the pion condensed phase, when $\frac{\mu_B}{3} = M_u - \frac{2}{3}m_\pi$. Using the constituent quark mass in the vacuum, $M_{u,d} = 325$ MeV for our parameter set, we find $\frac{\mu_B}{3} = 232$ MeV.

The line of second order phase transition eventually ends up in a critical point from which on the transition becomes first order. To demonstrate this, we plot in Fig. 6 the values of the condensates, the charge chemical potentials, and the in-medium pion mass (obtained as the pole of the pion propagator [20]) along the section of the phase diagram with $\mu_{L_e} = 400$ MeV for the $n_{L_\mu} = 0$ case and $\alpha = 0$. We observe that as α decreases, the critical point moves down and the pion-condensed phase shrinks to somewhat smaller μ_B. This is because small α tends to split the constituent masses of up and down quarks and thus disfavor the pairing mechanism which underlies the pion condensation.

IV. PION PROPERTIES IN A NEUTRINO GAS

As we saw in the previous sections, the lepton medium induces an isospin chemical potential. This chemical potential and the finite density of neutrinos will modify the behavior of the pions. Let us therefore have a closer look at the spectral properties of the pions in the lepton medium, in particular their masses and decay rates.

A. Masses

As long as the isospin is not spontaneously broken (i.e., there is no pion condensate), the in-medium pion masses are simply given by $M_{\pi^\pm} = m_\pi \mp \mu_Q$ [1, 2]. The pion condensation sets in where one of the masses drops to zero.

At low μ_{L_e}, only electrons are light enough to be excited. In order to preserve electric neutrality, we have to make sure that the electron chemical potential is zero, that is, $\mu_Q = \mu_{L_e}$. The pion masses are thus simply equal to $M_{\pi^\pm} = m_\pi \mp \mu_{L_e}$. When μ_{L_e} exceeds the muon mass, neutrality becomes a nontrivial issue and the pion masses depend on the exact way it is imposed. We will describe in detail two special cases: Zero muon lepton number chemical potential, and zero muon lepton number density, both of which were already discussed in Sec.

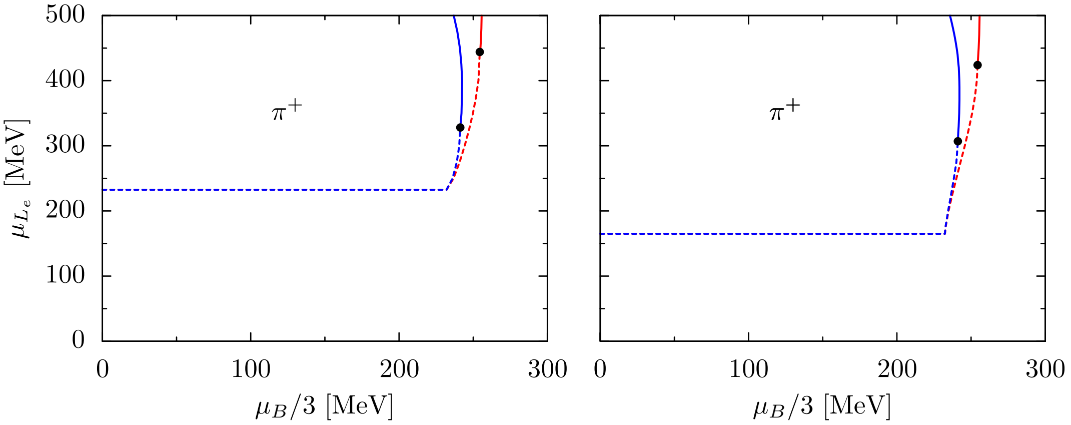

FIG. 5: Phase diagram of the electrically neutral NJL model in the $\mu_B - \mu_{L_e}$ plane at $T = 0$. Left panel: The $\mu_{L_\mu} = 0$ case. Right panel: The $n_{L_\mu} = 0$ case. The solid and dashed lines denote first and second order phase transitions, respectively. In each plot we display two curves corresponding to $\alpha = 0$ (left, blue) and $\alpha = 1/2$ (right, red). The black dots correspond to critical points.

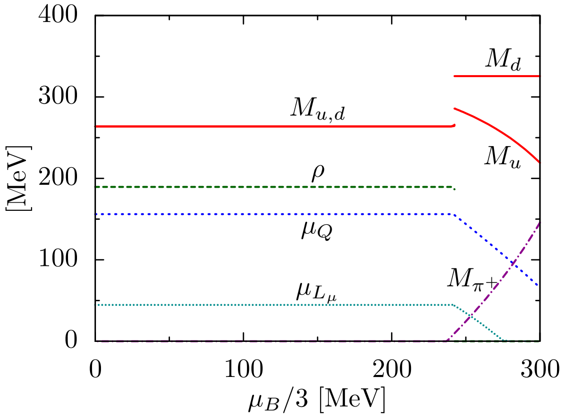

FIG. 6: Evolution of the condensates, chemical potentials and the in-medium pion mass as a function of μ_B for $\mu_{L_e} = 400$ MeV, $\alpha = 0$ and $T = 0$ in the $n_{L_\mu} = 0$ case.

II.

At $\mu_{L_\mu} = 0$ we have $\mu_{\mu^\pm} = \pm\mu_Q$ so that for $\mu_{L_e} > m_\mu + m_e$, antimuons will appear in the system. In this case electric neutrality requires that the electrons and antimuons have the same Fermi momentum, which leads to

$$\mu_Q = \frac{\mu_{L_e}^2 + m_\mu^2 - m_e^2}{2\mu_{L_e}}. \tag{26}$$

Setting $\mu_Q = m_\pi$ recovers the transition point to the pion condensed phase, Eq. (11).

If we instead demand zero muon lepton number density, the μ^+ chemical potential modifies to $\mu_Q - \mu_{L_\mu}$ and μ_{L_μ} is determined self-consistently from the muon lepton number neutrality condition; a negative contribution from antimuons has to be compensated by a finite density of muon neutrinos. Solving the set of two neutrality equations, we obtain the results shown in Fig. 3 by the dash-dotted lines. The mass of π^- is given simply by a reflection of the curves with respect to the $M = m_\pi$ line.

B. Decay rates

The charged pions in the vacuum decay predominantly in the $\pi^+ \to \mu^+\nu_\mu$, $\pi^- \to \mu^-\bar{\nu}_\mu$ channels. These constitute about 99.99% of the total decay rate [44]. In the vacuum and at rest, the decay rate is, at the leading order in weak interactions, given by the textbook formula

$$\Gamma_0 = \frac{1}{4\pi} V_{ud}^2 G_{\mathrm{F}}^2 f_\pi^2 m_\pi m_\mu^2 \left(1 - \frac{m_\mu^2}{m_\pi^2}\right)^2. \tag{27}$$

Here V denotes the Cabibbo–Kobayashi–Maskawa matrix and G_{F} the Fermi constant. The presence of the medium breaks explicitly Lorentz invariance, and we will therefore calculate the decay rates as a function of momentum. The derivation entails two ingredients which can be considered separately: The invariant decay amplitude and the kinematics.

To determine the invariant amplitude, we need to know the coupling of the pion to the charged weak current. In vacuum, this is equal to $\frac{i}{2} g V_{ud} f_\pi p^\mu$, where p^μ is the pion four-momentum and g the weak coupling constant. To determine how this is modified in the medium, we use chiral perturbation theory [45]. Introducing in the lowest order pion effective Lagrangian (22) the external vector electromagnetic as well as the left-handed charged weak current, we find that one simply has to make the replacement $p^\mu \to \tilde{p}^\mu = (p_0 + \mu_Q, \vec{p})$. In this simple estimate of the decay rate, we neglect truly quantum corrections to the pion decay constant which give it a weak medium dependence [46].

An explicit calculation shows that this change of the pion coupling to the weak current is precisely what is needed to make the total amplitude for the pion decay completely independent of the chemical potentials;

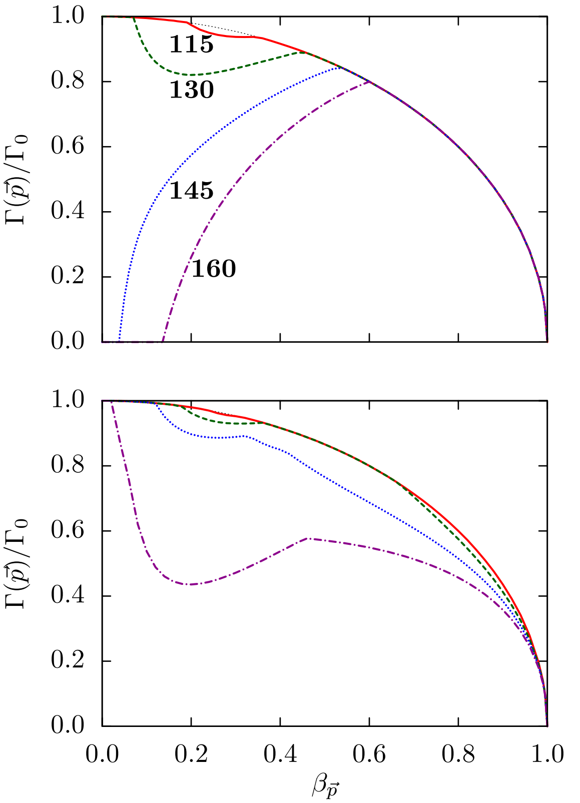

FIG. 7: Decay rate of π^+ in units of the vacuum rate at rest as a function of the pion velocity for various values of electron lepton number chemical potential (indicated by the numbers in boldface; the same values are implied in the lower plot). The thin dotted line indicates the vacuum decay rate, i.e., is trivially given by the γ-factor. Upper panel: The $\mu_{L_\mu} = 0$ case. Lower panel: The $n_{L_\mu} = 0$ case.

the extra term in the pion–weak-current coupling cancels with a similar term coming from the muon and neutrino wave functions. As a consequence the kinematics becomes trivial: The integration over phase space for the final state can be transformed into the center-of-mass frame (CMS). The only effect of the medium is a restriction of the phase space due to the fact that some of the momentum states are occupied by particles in the Fermi sea. The final formula for the decay rate as a function of momentum $\vec{p}$ then reads

$$\frac{\Gamma(\vec{p})}{\Gamma_0} = \frac{1}{\gamma_{\vec{p}}} \frac{\omega^*}{4\pi}, \tag{28}$$

where $\gamma_{\vec{p}}$ denotes the Lorentz factor and ω^* is the allowed solid angle for the products of the decay, measured in CMS.

First of all, observe the decay rate of π^- is trivially the same as in vacuum, because there are neither muons nor muon antineutrinos in the system. In the following we will therefore concentrate on the decay of π^+. In CMS the magnitude of the momentum of the antimuon and muon neutrino from the π^+ decay is

$$k_0 = \frac{m_\pi^2 - m_\mu^2}{2m_\pi}; \tag{29}$$

the decay is isotropic. (Note that since both the electric charge and the lepton number are preserved in the decay, the presence of chemical potentials does not affect the energy and momentum conservation.) Therefore, when the Fermi momentum of both antimuons and neutrinos is smaller than k_0, the decay rate will be Γ_0, otherwise it will be zero, at least for the considered process.

The energies of the antimuon and the neutrino in the rest frame of the medium are given by a simple Lorentz boost,

$$\epsilon_\mu = \gamma_{\vec{p}}(\epsilon_0 + \beta_{\vec{p}} k_0 \cos\theta^*), \quad \epsilon_\nu = \gamma_{\vec{p}} k_0 (1 - \beta_{\vec{p}} \cos\theta^*), \tag{30}$$

where $\beta_{\vec{p}}$ denotes the velocity. Furthermore, $\epsilon_0 = (m_\pi^2 + m_\mu^2)/(2m_\pi)$ is the antimuon energy and θ^* the angle of the antimuon with respect to the pion momentum, both measured in CMS. This allows a straightforward determination of the available phase space for the decay. For instance, in the case $\mu_{L_\mu} = 0$, only phase space blocking by antimuons occurs (there are no muon neutrinos) and one may explicitly express ω^* as

$$\frac{\omega^*}{4\pi} = \frac{1}{2}\left[1 - \Xi\left(\frac{1}{\beta_{\vec{p}} k_0}\left(\frac{\mu_Q}{\gamma_{\vec{p}}} - \epsilon_0\right), -1, +1\right)\right], \tag{31}$$

where the value of the function $\Xi(x, a, b)$ with $a < b$ is equal to a if $x < a$, to b if $x > b$, and to x otherwise, that is, $\Xi(x, a, b) = \min[\max(x, a), b]$.

The numerical results for the decay rate as a function of the pion velocity are shown in Fig. 7. The interpretation of the results is simple. If the chemical potentials are low enough such that the decay is not blocked in CMS, then boosting to finite momentum may bring the backward emitted particles into the Fermi sea and thus suppress the decay rate beyond the simple γ-factor from time dilation. On the other hand, if the decay is Pauli-blocked in CMS, boosting to finite momentum may liberate the forward-emitted particles so that the decay becomes possible. In the $n_{L_\mu} = 0$ case parts of the phase space are blocked by both antimuons and muon neutrinos.

V. CONCLUSIONS

In this article we have shown that a positively charged pion condensate arises in electrically neutral matter at high neutrino and small baryon densities. We found that at zero temperature, zero baryon chemical potential, and zero muon lepton number density, the onset of pion condensation lies at an electron neutrino number density of 9.6×10^{-3} fm^{-3}.

For zero temperature we have obtained the phase diagram of electrically neutral QCD as a function of μ_{L_e} and μ_{L_μ}, valid for small baryon chemical potential,

$|\mu_B| \lesssim m_p - m_\pi$. We have estimated this phase diagram at higher temperatures. Comparison to model calculations with obtained using the NJL model show that up to about $T = 50$ MeV these estimates are very good.

Using the NJL model we also studied the behavior of the phase diagram as a function of baryon chemical potential and lepton number chemical potential. We found that the pion condensed phase arises up to $|\mu_B/3| \approx M - \frac{2}{3}m_\pi$, where M is the constituent quark mass in the vacuum.

Hence the main conclusion of this work is that the pion condensed phase makes up a large part of the phase diagram of electrically neutral QCD at finite lepton number chemical potential and small baryon chemical potential.

Acknowledgments

We would like to thank J.O. Andersen, D. Boer and D.H. Rischke for discussions. The work of H.A. and T.B. is supported by the Alexander von Humboldt Foundation. H.J.W. acknowledges the support of the Helmholtz Alliance Program of the Helmholtz Association, contract HA-216 ‘Extremes of Density and Temperature: Cosmic Matter in the Laboratory’.

[1] D. T. Son and M. A. Stephanov, Phys. Rev. Lett. **86**, 592 (2001).
[2] J. B. Kogut and D. Toublan, Phys. Rev. D **64**, 034007 (2001).
[3] M. Loewe and C. Villavicencio, Phys. Rev. D **67**, 074034 (2003); M. Loewe and C. Villavicencio, Phys. Rev. D **70**, 074005 (2004); M. Loewe and C. Villavicencio, Phys. Rev. D **71**, 094001 (2005).
[4] J. B. Kogut and D. K. Sinclair, Phys. Rev. D **66**, 034505 (2002).
[5] Y. Nishida, Phys. Rev. D **69**, 094501 (2004).
[6] J. B. Kogut and D. K. Sinclair, Phys. Rev. D **70**, 094501 (2004).
[7] P. de Forcrand, M. A. Stephanov and U. Wenger, PoS **LAT2007**, 237 (2007).
[8] W. Detmold, K. Orginos, M. J. Savage and A. Walker-Loud, Phys. Rev. D **78**, 054514 (2008).
[9] B. Klein, D. Toublan and J. J. M. Verbaarschot, Phys. Rev. D **68**, 014009 (2003).
[10] D. Toublan and J. B. Kogut, Phys. Lett. B **564**, 212 (2003).
[11] A. Barducci, R. Casalbuoni, G. Pettini and L. Ravagli, Phys. Rev. D **69**, 096004 (2004); A. Barducci, R. Casalbuoni, G. Pettini and L. Ravagli, Phys. Rev. D **71**, 016011 (2005).
[12] L. He and P. Zhuang, Phys. Lett. B **615**, 93 (2005).
[13] L. y. He, M. Jin and P. f. Zhuang, Phys. Rev. D **71**, 116001 (2005).
[14] H. J. Warringa, D. Boer and J. O. Andersen, Phys. Rev. D **72**, 014015 (2005).
[15] H. Mao, N. Petropoulos and W. Q. Zhao, J. Phys. G **32**, 2187 (2006).
[16] J. O. Andersen, Phys. Rev. D **75**, 065011 (2007).
[17] A. Parnachev, JHEP **0802**, 062 (2008).
[18] J. Erdmenger, M. Kaminski, P. Kerner and F. Rust, JHEP **0811**, 031 (2008).
[19] A. Rebhan, A. Schmitt and S. A. Stricker, JHEP **0905**, 084 (2009).
[20] H. Abuki, R. Anglani, R. Gatto, M. Pellicoro and M. Ruggieri, Phys. Rev. D **79**, 034032 (2009).
[21] D. Ebert and K. G. Klimenko, J. Phys. G **32**, 599 (2006); D. Ebert and K. G. Klimenko, Eur. Phys. J. C **46**, 771 (2006).
[22] J. O. Andersen and L. Kyllingstad, arXiv:hep-ph/0701033.
[23] A. B. Migdal, Sov. Phys. JETP **34**, 1184 (1972).
[24] R. F. Sawyer, Phys. Rev. Lett. **29**, 382 (1972).
[25] D. J. Scalapino, Phys. Rev. Lett. **29**, 386 (1972).
[26] D. B. Kaplan and A. E. Nelson, Phys. Lett. B **175**, 57 (1986).
[27] J. A. Pons, S. Reddy, P. J. Ellis, M. Prakash and J. M. Lattimer, Phys. Rev. C **62**, 035803 (2000).
[28] D. T. Son and M. A. Stephanov, Phys. Rev. D **61**, 074012 (2000)
[29] T. Schafer, Phys. Rev. Lett. **85**, 5531 (2000).
[30] A. W. Steiner, S. Reddy and M. Prakash, Phys. Rev. D **66**, 094007 (2002).
[31] M. M. Forbes, Phys. Rev. D **72**, 094032 (2005).
[32] M. Buballa, Phys. Lett. B **609**, 57 (2005).
[33] H. J. Warringa, arXiv:hep-ph/0606063.
[34] J. O. Andersen and L. E. Leganger, arXiv:0810.5510 [hep-ph].
[35] T. H. Phat, N. V. Long, N. T. Anh and L. V. Hoa, Phys. Rev. D **78**, 105016 (2008).
[36] M. Prakash, I. Bombaci, M. Prakash, P. J. Ellis, J. M. Lattimer and R. Knorren, Phys. Rept. **280**, 1 (1997).
[37] M. Buballa, Phys. Rept. **407**, 205 (2005).
[38] C. Ratti, M. A. Thaler and W. Weise, Phys. Rev. D **73**, 014019 (2006)
[39] Z. Zhang, K. Fukushima and T. Kunihiro, Phys. Rev. D **79**, 014004 (2009).
[40] M. Frank, M. Buballa and M. Oertel, Phys. Lett. B **562**, 221 (2003).
[41] S. B. Rüster, V. Werth, M. Buballa, I. A. Shovkovy and D. H. Rischke, Phys. Rev. D **73**, 034025 (2006).
[42] V. Laporta and M. Ruggieri, Phys. Lett. B **633**, 734 (2006).
[43] F. Sandin and D. Blaschke, Phys. Rev. D **75**, 125013 (2007).
[44] C. Amsler *et al.* [Particle Data Group], Phys. Lett. B **667**, 1 (2008).
[45] S. Scherer, Adv. Nucl. Phys. **27**, 277 (2003).
[46] A. Barducci, R. Casalbuoni, S. De Curtis, R. Gatto and G. Pettini, Phys. Rev. D **42**, 1757 (1990).